An Ultra-Low Phase-Noise 20-GHz PLL Utilizing an Optoelectronic Voltage-Controlled Oscillator

Aaron Bluestone, *Student Member, IEEE*, Daryl T. Spencer, *Student Member, IEEE*, Sudharsanan Srinivasan, *Student Member, IEEE*, Danielle Guerra, John E. Bowers, *Fellow, IEEE*, and Luke Theogarajan, *Member, IEEE*

***Abstract*—This paper describes a novel phase-locked loop (PLL) architecture utilizing an optoelectronic oscillator (OEO) as a voltage-controlled oscillator (VCO). The OEO demonstrates excellent far-out phase-noise performance while the PLL reduces the close-in phase noise. The nonmonotonic VCO characteristics of the OEO placed stringent demands on the loop filter electronics and startup conditions. The crystal reference, prescalar, frequency synthesizer, and loop filter were all implemented with discrete high-performance components. The resulting frequency synthesizer yields a −10-dBm output at 20 GHz with phase noise of −80 dBc/Hz at 100-Hz offset, and −134 dBc/Hz at 10-kHz offset. These results are far superior to PLL synthesizers utilizing only an electronic VCO and illustrate the power of optoelectronic integration.**

***Index Terms*—Frequency stability, low phase noise, optoelectronic oscillators (OEOs), phase-locked loops (PLLs).**

I. Introduction

K-BAND oscillators are essential to a growing number of applications in metrology, wireless communications, and high-speed sampling [1]–[3]. All these microwave systems demand a spectrally pure reference for precise knowledge of frequency and phase information. At such high frequencies, electronic oscillators suffer from parasitic losses, decreasing the quality factor and increasing close to carrier phase noise, which degrades the signal-to-noise ratio. Direct up-conversion of stable oscillators at low frequencies suffer from a $20 \times \log_{10}(N)$ increase in phase noise for a multiplication factor of N. Thus, high-frequency sources with extremely low phase noise are needed. While low-frequency quartz oscillators exhibit very low close-in phase noise due to their high thermal stability, the far out performance is not on-par with optoelectronic oscillators (OEOs). OEOs utilize the low loss of optical fibers to achieve microwave quality factors higher than those achievable in the electrical domain at high frequencies [4]. This makes OEOs suitable for numerous applications including frequency multiplication, pulse and comb frequency generation, and clock and carrier recovery [5]. The optimal solution in designing an ultra-low phase noise frequency synthesizer, operating at microwave frequencies, should utilize up-conversion for close-in performance while benefiting from the OEO's far-out performance. Previous works have demonstrated locking a microwave source to a laser in a phase-locked loop (PLL) configuration for applications in electrooptic sampling [6]. We present a dual-loop OEO operating at 20 GHz stabilized with multiple techniques in the optical domain. The OEO was further stabilized by electronically phase locking it to a low-frequency reference for long-term stability, a region in which OEOs usually suffer due to fiber drift, by operating the OEO as a voltage-controlled oscillator (VCO) within a PLL. Though OEOs operating as VCOs in a PLL configuration have been shown [7], they do not discuss the challenges or the solutions to the challenges posed by the nonidealities of an OEO operating as a VCO. Optical mode-hopping and the fiber loop delay define both a tight pull-in range and start-up conditions for phase locking, which is not usually the case in a conventional PLL loop, requiring additional start-up circuitry.

This paper is organized as follows. First we describe the dual-loop OEO and the optimizations made to achieve ultra-low phase noise. Following this, the PLL design will be discussed. Next, the experimental results will be presented, and finally, we will conclude this paper along with a discussion of future work.

II. OEO System Design

The OEO generates spectrally pure microwave tones through the use of an optical resonator with electronic feedback. In the optical section, the output of a high power fiber laser passes through an intensity modulator, fiber delay, and is detected on a high-speed photodetector (PD). The frequency of oscillation of the electrical signal from the PD is selected with a microwave filter, and any required amplifiers and phase shifter are added before closing the microwave loop to the intensity modulator. The main advantages of the OEO architecture are the tunability of microwave frequency with a microwave phase shift, and the long delay times achievable due to low optical propagation losses (0.2 dB/km). The longest delay of 10 km used in this study can produce effective microwave quality factors of 10 billion. However, the noise performance is degraded by flicker noise produced by other components. The free spectral range (FSR) of the loop becomes very narrow (20 kHz)

Manuscript received June 18, 2014; revised December 15, 2014; accepted January 16, 2015. Date of publication February 13, 2015; date of current version March 03, 2015.

The authors are with the Department of Electrical and Computer Engineering, University of California at Santa Barbara, Santa Barbara, CA 93106-9560 USA (e-mail: aaronjbluestone@ece.ucsb.edu; darylt@ece.ucsb.edu; sudhas@ece.ucsb.edu; dmguerra@ece.ucsb.edu; bowers@ece.ucsb.edu; ltheogar@ece.ucsb.edu)

Color versions of one or more of the figures in this paper are available online at http://ieeexplore.ieee.org.

Digital Object Identifier 10.1109/TMTT.2015.2397890

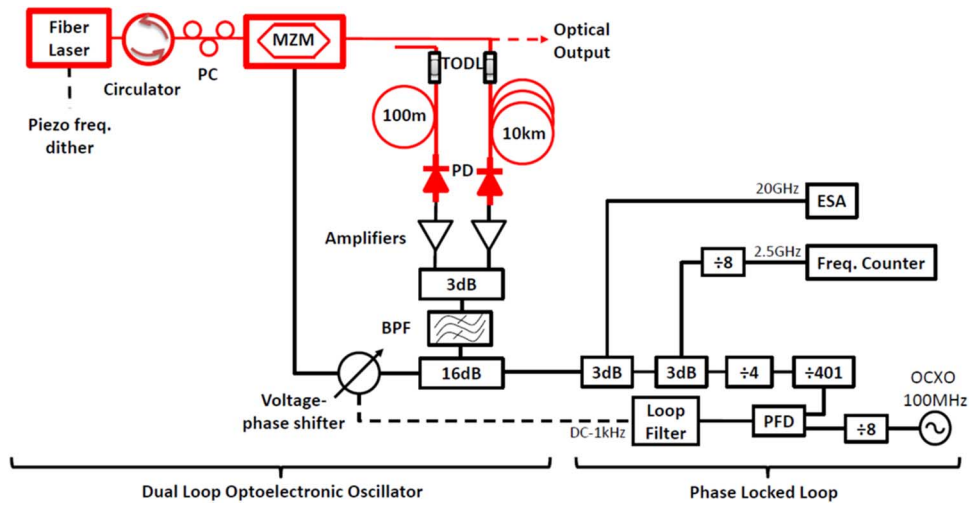

Fig. 1. Schematic of the dual-loop OEO (*left*) utilized as a VCO for PLL feedback (*right*). The fiber laser output is controlled with a polarization controller (PC) before being sent to a Mach–Zender modulator (MZM). Tunable optical delay lines (TODLs) control the Vernier effect, and the photodetectors (PDs) generate the microwave signal sent through the bandpass filter (BPF). After frequency division, the phase frequency detector (PFD) compares the dual-loop OEO noise to an oven controlled crystal oscillator (OCXO), and sends the feedback signal to the OEO.

with such long lengths requiring additional filtering for mode selection and spurious tone suppression. The dual-loop OEO, introduced by Yao *et al.* [8], is one of the many techniques [9], [10] to suppress supermode noise generated from the long optical delay lines in an OEO. This oscillator provides a narrow microwave linewidth and good frequency stability without mode hopping simultaneously. Additionally this oscillator relaxes the requirement of a 20-GHz microwave filter with sub-megahertz linewidths.

The dual-loop OEO is shown on the left side of Fig. 1. The optical source is a 1556-nm fiber laser whose linewidth and relative intensity noise (RIN) are 120 kHz and -140 dB/Hz, respectively. The frequency noise of the laser is the dominant contribution to microwave phase noise due to the dispersion of fiber, as described in [11]. The OEO is known to be highly sensitive to reflections reaching the laser, and the intracavity optical power can become limited by fiber scattering [12]. We added a fiber circulator after the high-power fiber laser to circumvent the first issue and broaden the fiber linewidth by dithering the built in piezo frequency tuner to overcome the second problem. The 20-GHz intensity modulator has a V_π of 3.8 V and insertion loss of 2.5 dB. The dc bias point is placed near quadrature and optimized for maximum RF power. The maximum optical input power to the modulator is also limited to 100 mW, rendering the use of high input powers to lower phase noise infeasible.

The tuning range of this oscillator is dictated by the shorter of the two fiber delay lines while the tuning resolution is determined by the longer fiber spool. In our case, we used 100 m and 10 km as the two delay lengths, which correspond to a tuning range of $\sim$2 MHz and a tuning resolution of $\sim$20 kHz. We have included two tunable optical delay lines (TODLs) on each arm to provide continuous tuning between the 20-kHz modes. This enabled the precise tuning of the microwave oscillation frequency to within a few hundred hertz of the oven controlled crystal oscillator (OCXO). The tunable delay lines have a tuning range of 100 mm and a tuning resolution of 318 μm per screw

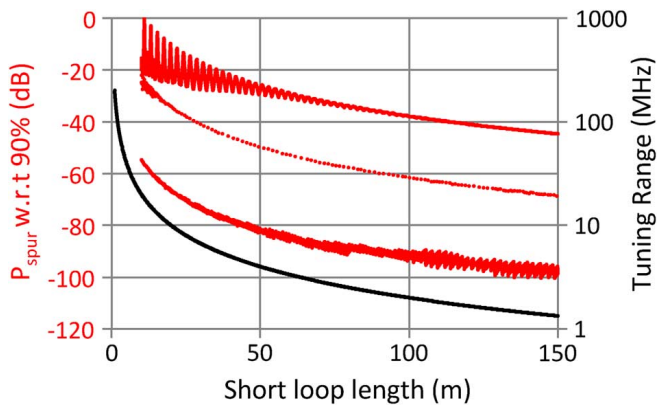

Fig. 2. Relative suppression of the nearest spur mode versus short loop length, corresponding to different powers launched into the long fiber delay. 90% (dashed), 50% (dotted), and 10% (solid). The tuning range (solid black line) is also shown.

turn. These numbers correspond to a frequency tuning range and tuning resolution as dictated by the following expression:

$$\frac{\Delta f}{f} = -\frac{\Delta L_1}{L_1} = -\frac{\Delta L_2}{L_2} \tag{1}$$

where f is the microwave oscillation frequency. The enhanced supermode noise suppression in the dual-loop OEO comes from the vernier effect of the oscillating modes in each loop. This suppression is important to increase the OEO stability since mode hopping will not occur for small perturbations to the system. The choice of the short fiber length is made based on the plot shown in Fig. 2. The plot shows the compromise in tuning range of the oscillator for better suppression of the nearest $\sim$20-kHz mode. For lengths longer than 100 m, the sharp resonances, which arise when the mode spacing of the short loop is an integer multiple of the mode spacing of the long loop, are avoided.

The two delay lines are terminated on 50-GHz u2t PDs (Finisar XPDV-2120R) with a responsivity of 0.55 A/W and maximum microwave output power of ∼5 dBm. Two low-noise microwave amplifiers with 42 dB of gain are placed directly after the PDs to keep the open-loop noise figure low. This is followed by a microwave power combiner with an excess loss of 1 dB for each arm. A 20-GHz filter with a 400-MHz full width at half maximum (FWHM) is used to select the oscillating frequency regime. Finally, a voltage-controlled analog phase shifter is inserted for microwave frequency tunability. The phase shifter has 2π phase shift over 7.3 V, and is used as the feedback element of the PLL circuit, to be described later.

The resulting short-term linewidth of the microwave signal is in the sub-hertz level, but a major issue with fiber delays is the dn/dT $1.2\times10^{-5}/^{\circ}$C associated with thermal fluctuations [7]. A change in the optical path length from temperature drift will cause the 20.05-GHz oscillating frequency to shift, which we observed to be ∼1 kHz/min. We reduced this to ∼200 Hz/min by placing the system in a sealed anechoic enclosure with a stabilization time of 5 h. Further stabilization was performed using the PLL loop discussed below.

III. PLL System Design

To further reduce the long-term linewidth (or close in phase noise), we have implemented a PLL that utilizes the dual-loop OEO as a VCO. As shown on the right side of Fig. 1, the PLL divides the 20.05-GHz output to a digital 12.5-MHz signal. A phase-frequency detector (PFD) then compares the OEO to an OCXO, and sends a filtered correction signal to the voltage controlled microwave phase shifter within a 1-kHz bandwidth.

An oven-controlled dual-frequency module with 10/100-MHz coupled outputs (NEL Frequency Controls) was chosen as the reference for its close-in phase-noise performance. The 100-MHz output achieves −125 dBc/Hz at 10-Hz offset and −160 dBc/Hz at 1-kHz offset. Most commercial frequency synthesizers only accept input frequencies less than 8 GHz. For this reason, the OEO output is first passed through a Hittite HMC447 divide-by-4 prescalar. The 5-GHz output is then sent to an integer-N synthesizer along with the OCXO reference. The ADF4108 frequency synthesizer was chosen for its tunable divide ratios in the VCO and reference paths, precision charge pump output, and low PFD noise floor of −223 dBc/Hz (normalized). The charge pump current is converted to the VCO feedback voltage through a passive first-order loop filter.

The synthesizer requires the VCO to lock to an integer multiple of the PFD frequency. Since the OCXO only has a tuning range of +/−50 Hz, this necessitates an optical mode within 10 kHz of a PFD multiple. Once the closest optical mode is chosen, the TODLs are adjusted to place the output frequency at the exact multiple, as discussed in the previous section. The optical loop has slightly higher gain at 20.05 GHz than the rest of the bandwidth and consequently tends to excite stable modes nearby, and thus, has been chosen as the mode of choice. Currently the OCXO has a divide-by-8, leading to a PFD comparison at 12.5 MHz. An integer division of 401 along with the prescalar divide-by-4 aligns with the desired VCO frequency of 20.05 GHz.

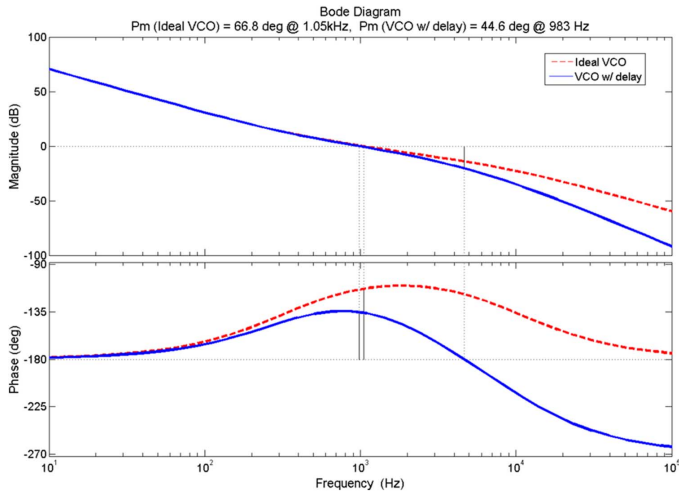

Fig. 3. PLL open-loop transfer function. This shows a phase margin comparison between an ideal VCO and the OEO VCO with fiber delay.

The nature of the optics in the VCO prevents it from being treated as an ideal integrator for voltage to phase domain conversion. The 10-km fiber path gives a 50-μs time delay for any small signal applied on the VCO tuning voltage. A second-order Padé approximation models this in the frequency domain as

$$\frac{1-\frac{\tau}{2}s+\frac{\tau^2}{12}s^2}{1+\frac{\tau}{2}s+\frac{\tau^2}{12}s^2} \tag{2}$$

where τ is the 50-μs time delay [13]. The loop was designed for a 1-kHz bandwidth and 66.8° phase margin to stay well beneath that additional pole and provide ample stability. After the fiber delay was taken into account, the loop bandwidth change was negligible while the phase margin degraded to 44.6°, as shown in Fig. 3. This corresponds to a 33% overshoot for a closed-loop step response, and requires significant consideration when attempting to lock the loop. A time-to-digital converter (TDC) and a digital loop filter could be used in the future to account for this delay, improving our loop bandwidth and further reducing phase noise [14].

The optical loop has hundreds of stable oscillating modes surrounding 20 GHz. Sweeping the VCO tuning voltage across its full range leads to several optical mode hoppings, each causing a large jump in the output RF frequency. A typical operating point will allow +/−0.25-V change before an optical mode hop. The effect of this limit can be found by analyzing the step response of the PLL and ensuring the maximum change in the control voltage is limited to 0.5 V about the operating point. Paired with the 33% overshoot described earlier, the PLL is limited to an 800-Hz pull-in range. In order to switch on the feedback loop from a reset state, the integrator must remain discharged while a stable dc operating point is found. This was accomplished with a resettable loop filter and noninverting summer, as shown in Fig. 4.

IV. Measurement Methods

Three measurement methods were employed to characterize the performance of the OEO. Phase noise gives a measurement

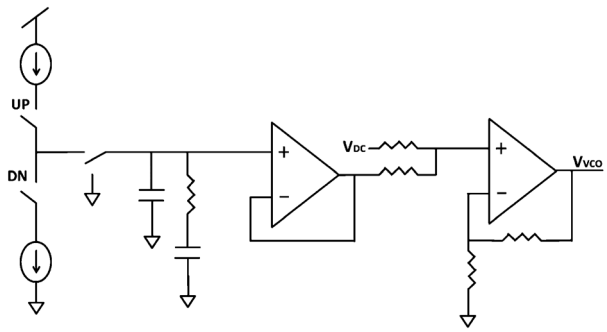

Fig. 4. Loop filter and noninverting summer in feedback path. The loop filter input is toggled between a ground reset and the charge-pump input via a single-pole double-throw switch.

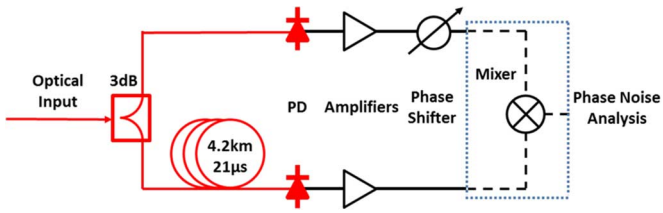

Fig. 5. Schematic of the optical frequency discriminator used to measure the phase noise of the OEO.

of short-term (<1 s) phase fluctuations at multiple carrier offset frequencies. The ESA (Rhode & Schwarz FSU50) provides the most straightforward method of measuring phase noise, as it has an internal synthesizer, reference oscillator, and tunable filters for a large measurement of offset frequencies from 1 Hz to the Nyquist rate. To obtain more sensitive measurements at certain offset frequencies, a carrier suppressed frequency discriminator technique is used [15], [16]. Carrier suppression techniques rely on two identical frequencies entering a mixer in which one input is biased at $\pi/2$ phase shift relative to the second input. The resulting baseband PSD with filtered harmonics is the combination of the two inputs' phase noises. The two inputs can be two noncorrelated oscillators, or the same signal, with one being time delayed as in the case of the frequency discriminator. As shown in Fig. 5, we use the optical frequency discriminator to split the OEO's optical output and delay one arm in a 4.2-km fiber spool. The two arms are detected on high-speed PDs and amplified by 40 dB to obtain two strong microwave signals to drive the mixer. Using low noise-figure amplifiers allows for a similar white phase-noise floor in the discriminator as inside the OEO. A passive phase shifter is used on one arm to bias it at a relative $\pi/2$ phase shift. The two inputs go to the Agilent E5505A system, which includes the mixer, low-frequency filters and amplifiers, and software analysis. The 4.2-km frequency discriminator provides a reliable measurement up to an offset frequency of 48 kHz, where a measurement spur will be located.

The third measurement method to characterize the OEO performance is the Allan deviation (ADEV). A frequency counter is used to compare the zero crossings of a signal and reference to obtain the frequency to certain digit accuracy. After recording a time series of frequency measurements for a given gate time,

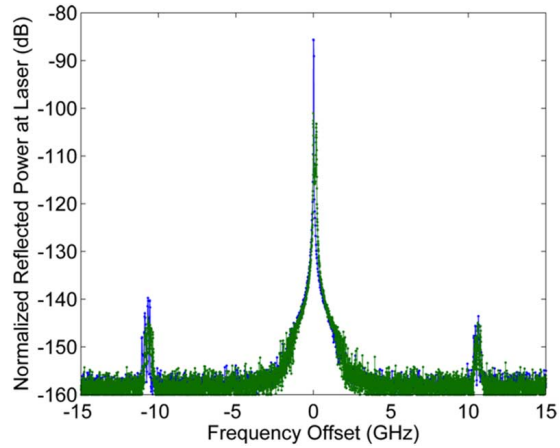

Fig. 6. Normalized reflected optical power reaching the fiber laser, as measured on the third port of the optical circulator with (green in online version) and without (blue in online version) 46-kHz dither. The laser output power is 20 dBm and the optical isolation is 50 dB. The resolution bandwidth of the OSA is 20 MHz.

the frequency deviation from the mean, $\Delta f/f$, is plotted for different averaging times to obtain the ADEV. We use a 12-digit microwave counter (Keysight 53230A) to measure the OEOs microwave frequency after being divided by 8. An isolated external OCXO is used as the timing reference to the frequency counter.

V. Results

A. OEO Results

To quantify the amount of reflection reaching the fiber laser, we measure the optical spectrum on the third port of the circulator. After normalizing the output power of 20 dBm and 50 dB of optical isolation, Fig. 6 plots the results versus offset from the laser frequency. As we apply the 46-kHz frequency dither, we observe a 15-dB decrease in the Rayleigh backscatter at the laser frequency, from -85 to -100 dB, but no change in the Brillouin backscatter level at 10.8 GHz, -140 dB. We have avoided high optical powers in the fiber delays such that Brillouin nonlinearities would not limit the achievable intracavity power.

The expression for the power spectral density of the microwave output of the dual-loop OEO is given by [17]

$$P(\omega) \infty \left| \frac{1}{1-(g_1 e^{j\omega\tau_1} + g_2 e^{j\omega\tau_2})} \right|^2 \tag{3}$$

where g_1, g_2 and τ_1, τ_2 are the individual voltage gains and time delays of the two loops, respectively. The condition for oscillation is given by $|g_1| + |g_2| = 1$ and $|g_1| = |g_2| = 0.5$ when the roundtrip microwave gain in both loops is greater than or equal to unity. We investigated the situation for cases when one of the two loops does not have enough gain to sustain oscillations by itself. The effect is the two loops do not contribute equally in the expression shown in (3). Using the technique described in [17], we evaluate the phase noise (Ψ) of the microwave signal

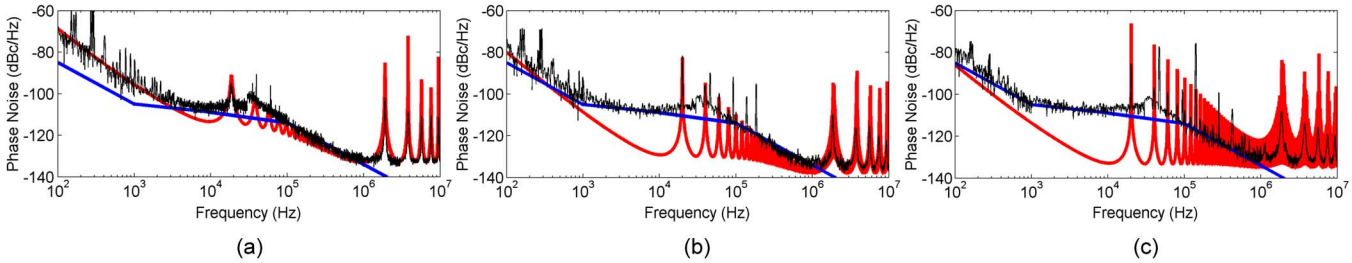

Fig. 7. Measured (black) and modeled (red in online version) phase noise of the dual-loop OEO for different powers launched into the longer fiber loop. (a) 10%. (b) 50%. (c) 90%. The blue line (in online version) is a guide to the eye showing the specified noise floor of the ESA. The values of D_m, D_a, ω_l, and ω_h used for fitting are 5×10^{-13} rad^2/Hz, 3.162×10^{-15} rad^2/Hz, 1 rad/s, and 90×10^5 rad/s, respectively.

when loop gain in one of the two loops is less than unity, shown as follows:

$$|\Psi(\omega)|^2 = \left| \mu \frac{(2Q)^{-1}\eta_m(\omega) + |A_0|^{-1}\xi_a(\omega)}{j\omega + \mu\left(1 - \left[\frac{\gamma_1 J_{C1}(|A_1|)e^{-j\omega\tau_1} + \gamma_2 J_{C1}(2|A_2|)e^{-j\omega\tau_2}}{\gamma_1 J_{C1}(2|A_1|) + \gamma_2 J_{C1}(2|A_2|)}\right]\right)} \right| \quad (4)$$

where $\mu = \Delta\Omega/\sqrt{1+(1/2Q)^2}$, $\Delta\Omega$ and Q are the FWHM and the quality factor of the RF filter. ω is the offset frequency and $J_{C1}(x) = J_1(x)/x$, where $J_1(x)$ is the first-order Bessel function. η_m and ξ_a are the multiplicative and additive noise terms, as described in [18], $|A_0|$, $|A_1|$ and $|A_2|$ are the voltage amplitudes of the microwave oscillation at the modulator input and inputs to the microwave power combiner, respectively. τ_1, τ_2 are the time delays and γ_1, γ_2 are the total roundtrip voltage gain/loss for the two loops.

We measured the phase noise of the OEO for three different power splitting ratios between the two loops. The measured and fitted data is shown in Fig. 7. Fig. 7(a)–(c) corresponds to 10%, 50%, and 90% of the output power from the modulator coupled to the longer fiber delay. The model fits well with the data; however, the noise floor of the ESA prevents a continuous fit. For smaller powers in the long delay line, the spurs are significantly lower and slightly blue shifted in frequency. However, the close-in phase noise increases by 20 dB because the linewidth reduction is less pronounced. The noise at the frequency modulation rate of the laser (46 kHz) and its harmonics also increases with increasing launch power in the long optical fiber because of increased intensity of the doubly Rayleigh scattered light interfering with the principle laser light. We select the configuration with 90% of the optical power in the longer 10-km loop to achieve low close in phase noise and reasonable side-mode suppression.

B. PLL Results

The phase-noise measurements from the ESA and frequency discriminator are shown in Fig. 8. Using the ESA, the white phase-noise floor is -138 dBc/Hz, limited by the laser RIN and thermal noise of our microwave amplifiers. We have measured an optical link gain (modulator input to detector output) of -30 dB$_{\mathrm{RF}}$. Using the calculated thermal (-145 dBc/Hz), shot (-163 dBc/Hz), and RIN (-143 dBc/Hz) noise powers of each loop after the microwave combiner yields a theoretical white

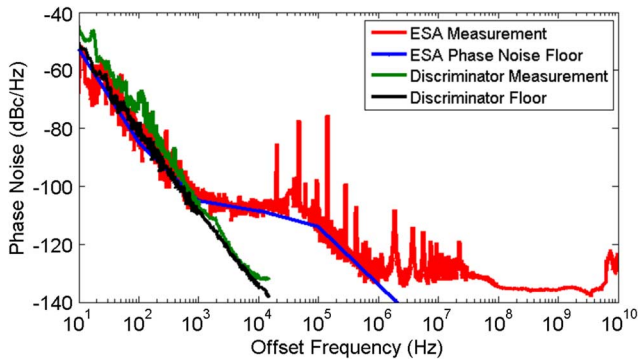

Fig. 8. Phase-noise spectrum of the dual-loop OEO as measured by the ESA and 4.2-km optical frequency discriminator.

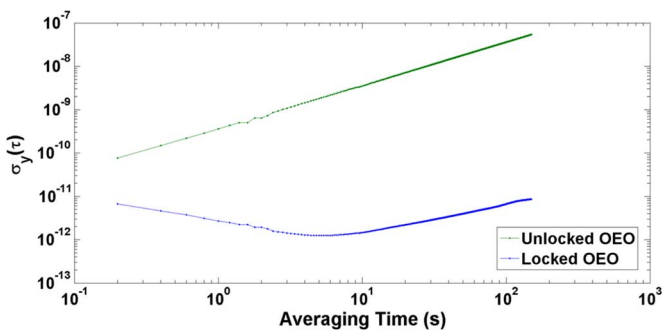

Fig. 9. Overlapping ADEV of the dual-loop OEO, measured at 2.5 GHz.

phase noise floor of -141 dBc/Hz. Theoretically the thermal noise floor can be further reduced with higher optical powers, requiring low nonlinearity fibers. Using improved lasers, the RIN noise floor could be further decreased. At 200-MHz offset, spurious tones begin to appear inside the FWHM of the microwave filter in our system. The rise in phase noise at 1 MHz is due to the ESA's internal noise floor. We use the frequency discriminator measurement to show a phase noise of -134 dBc/Hz at 10 kHz with a $1/f^3$ slope. This is currently limited by the residual noise of our discriminator.

We also used a frequency counter with an OCXO reference to characterize the stability improvement of our PLL. Fig. 9 plots the ADEV of the temperature stabilized OEO in the unlocked and locked states. The unlocked oscillator shows frequency drift (τ) irrespective of averaging time (>200 ms), while the locked OEO experiences white frequency modulation ($\tau^{-1/2}$) for averaging times less than 5 s, and is limited by the frequency drift

of the PLL's OCXO reference beyond this point. The locked oscillator exhibits a stability of less than ten parts per trillion up to 100-s averaging time.

VI. Future Work

One of the main focuses moving forward will be to develop a measurement system for recording lower phase noise. One option is to develop a second OEO as a noncorrelated oscillator for measuring phase noise on the Agilent E5505A. This would be similar to the frequency discriminator method, but would avoid the added flicker noise of the discriminator's components.

We are also looking into designing a 20-GHz fractional-N synthesizer for this loop and similar applications. The divided-down OEO signal going into the PFD could be used as a separate output for measuring phase noise at a lower frequency. This integrated circuit (IC) would eliminate the need for TODLs and any stable operating point could be used with a fractional division to the PFD frequency. In addition, this would encompass the prescalar and resettable loop filter, shrinking the size and reducing noise contribution.

An eventual goal will be to co-integrate the electronics and photonics onto a single chip, using high-Q resonators as delay elements. Similar work by Chen *et al.* has shown this should provide excellent environmental stability, decreased size, and lower power consumption [19].

VII. Conclusion

We have demonstrated a low phase-noise dual-loop OEO operating in the K-band. To achieve low noise and stable performance, multiple tactics have been applied to the basic OEO architecture. Fiber scattering, spurious tones, and mode-hopping effects have been decreased through linewidth broadening and adding a second fiber loop. To increase the long-term stability, we have implemented a PLL to transfer the parts per billion stability of a low-frequency OCXO to the high-frequency dual-loop OEO. The challenges in operating the dual-loop OEO as a VCO were overcome with optical path tuning control and custom startup circuitry in the feedback path.

Acknowledgment

The authors thank J. Conway, M. Heck, G. Fish, E. Norberg, and L. Johansson for helpful discussions.

References

[1] *Proceedings of the 7th Symposium: Frequency Standards and Metrology*, L. Maleki, Ed.. Pacific Grove, CA, USA: World Sci., 2008.

[2] J. A. Scheer, "Coherent radar system performance estimation," in *Proc. Radar Conf.*, Arlington, VA, USA, May 7–10, 1990, pp. 125–128.

[3] R. H. Walden, "Analog-to-digital converter survey and analysis," *IEEE J. Sel. Areas Commun.*, vol. 17, no. 4, pp. 539–550, Apr. 1999.

[4] X. S. Yao, L. Maleki, and D. Eliyahu, "Progress in the opto-electronic oscillator—A ten year anniversary review," in *IEEE MTT-S Int. Microw. Symp. Dig*, 2004, pp. 287–290.

[5] X. S. Yao and L. Maleki, "Optoelectronic oscillator for photonic systems," *IEEE J. Quantum Electron.*, vol. 32, no. 7, pp. 1141–1149, Jul. 1996.

[6] H. H. Wu, G. R. Lin, and C. L. Pan, "Optoelectronic phase tracking and electrooptic sampling of free-running microwave signals up to 20 GHz in a laser-diode-based system," *IEEE Photon. Technol. Lett.*, vol. 7, no. 6, pp. 670–672, Jun. 1995.

[7] D. Eliyahu, K. Sariri., A. Kamran, and M. Tokhmakhian, "Improving short and long term frequency stability of the opto-electronic oscillator," in *Freq. Control Symp. & PDA Exhibit.*, 2002, pp. 580–583.

[8] X. S. Yao, L. Maleki, and G. Lutes, "Dual-loop opto-electronic oscillator," in *Proc. IEEE Int. Freq. Control Symp.*, 1998, pp. 545–549.

[9] W. Zhou and G. Blasche, "Injection-locked dual optoelectronic oscillator with ultra-low phase noise and ultra-low spurious level," *IEEE Trans. Microw. Theory Techn.*, vol. 53, no. 3, pp. 929–933, Mar. 2005.

[10] K. H. Lee, J. Y. Kim, and W. Y. Choi, "Injection-locked hybrid optoelectronic oscillators for single-mode oscillation," *IEEE Photon. Technol. Lett.*, vol. 20, no. 19, pp. 1645–1647, Oct. 2008.

[11] K. Volyanskiy, Y. K. Chembo, L. Larger, and E. Rubiola, "Contribution of laser frequency and power fluctuations to the microwave phase noise of optoelectronic oscillators," *J. Lightw. Technol.*, vol. 28, no. 18, pp. 2730–2735, Sep. 2010.

[12] D. Eliyahu, D. Seidel, and L. Maleki, "RF amplitude and phase-noise reduction of an optical link and an opto-electronic oscillator," *IEEE Trans. Microw. Theory Techn.*, vol. 56, no. 2, pp. 449–456, Feb. 2008.

[13] G. H. Golub and C. F. Van Loan, *Matrix Computations*. Baltimore, MD, USA: The Johns Hopkins Univ. Press, 1989, pp. 557–558.

[14] A. Bonfanti, F. Amorosa, C. Samori, and A. L. Lacaita, "A DDS-based PLL for 2.4 GHz frequency synthesis," *IEEE Trans. Circuits Syst. II, Analog Digit. Signal Process.*, vol. 50, no. 12, pp. 1007–1010, Dec. 2003.

[15] O. Okusaga, "Photonic delay-line phase noise measurement system," ARL, Adelphi, MD, USA, Tech. Rep. ARL-TR-5791, 2011.

[16] "Phase noise characterization of microwave oscillator: frequency discriminator method," Agilent Technol., Santa Clara, CA, USA, Product Note 11729C-2, 2007.

[17] X. S. Yao and L. Maleki, "Multiloop optoelectronic oscillator," *IEEE J. Quantum Electron*, vol. 36, no. 1, pp. 79–84, Jan. 2000.

[18] Y. K. Chembo, K. Volyanskiy, L. Larger, E. Rubiola, and P. Colet, "Determination of phase noise spectra in optoelectronic microwave oscillators: A Langevin approach," *IEEE J. Quantum Electron*, vol. 45, no. 2, pp. 178–186, Feb. 2009.

[19] L. Chen, A. Sohdi, J. E. Bowers, L. Theogarajan, J. Roth, and G. Fish, "Electronic and photonic integrated circuits for fast data center optical circuit switches," *IEEE Commun. Mag.*, vol. 51, no. 9, pp. 53–59, Sep. 2013.

Aaron Bluestone (S'14) received the B.S. degree in electrical engineering from the University of California at Santa Barbara, Santa Barbara, CA, USA, in 2008, and is currently working toward the Ph.D. degree in electrical and computer engineering at the University of California at Santa Barbara.

His current research interest is in mixed-signal integrated-circuit design for optoelectronic applications.

Daryl T. Spencer (S'12) received the B.S. degree in engineering physics from the University of Tulsa, Tulsa, IL, USA, in 2010, the M.S. degree in electrical and computer engineering from the University of California at Santa Barbara, Santa Barbara, CA, USA, in 2012, and is currently working toward the Ph.D. degree in electrical and computer engineering at the University of Santa Barbara.

He is currently a National Science Foundation (NSF) Fellow with the University of Santa Barbara. His research involves the active integration of ultra-high quality factor monolithic resonators for high-performance microwave systems.

Sudharsanan Srinivasan (S'09) received the Bachelors degree (with a specialization in engineering physics) from the Indian Institute of Technology, Madras, India, in 2009, and is currently working toward the Ph.D. degree in electrical and computer engineering at the University of California at Santa Barbara, Santa Barbara, CA, USA.

His research interests are in silicon photonics.

Danielle Guerra received the B.S. and M.S. degrees in electrical engineering from the University of California at Santa Barbara, Santa Barbara, CA, USA, in 2010 and 2014, respectively, and is currently working toward the Ph.D. degree at the University of California at Santa Barbara.

From 2000 to 2006, she was in the U.S. Air Force, as a Facilities Maintenance Technician and Team Chief for intercontinental ballistic missiles with Malmstrom AFB. She also instructed and developed course material for new technicians at Vandenberg AFB. From 2012 to 2013, she interned with Aurrion Inc., where she developed high-speed system-level electronics–photonics simulations in MATLAB Simulink for developing insight into critical interactions between different physical domains. In the summer of 2013, she interned with Qualcomm, where she developed system-level analog–digital simulations in Cadence AMS for verification of control driver and power management integrated circuit (IC) designs for microelectromechanical systems (MEMs) visual displays designed for SHARP. Her research interests include a focus on system-level and IC-level electronic control between multiple physical domains such as photonic and biological interfacing. She is currently involved interfacing with protein-based bionanotechnology for the purpose of efficient DNA/RNA sequencing.

John E. Bowers (F'93) received the M.S. and Ph.D. degrees from Stanford University, Stanford, CA, USA.

He currently holds the Fred Kavli Chair in Nanotechnology, and is the Director of the Institute for Energy Efficiency and a Professor with the Departments of Electrical and Computer Engineering and Materials, University of California at Santa Barbara (UCSB), Santa Barbara, CA, USA. He is a cofounder of Aurrion, Aerius Photonics, and Calient Networks. He was with AT&T Bell Laboratories and Honeywell prior to joining UCSB. He has authored or coauthored 10 book chapters, 600 journal papers, and 900 conference papers. He holds 54 patents. He has also authored or coauthored 180 invited papers and conference papers and has given 16 plenary talks at conferences. He is primarily interested in optoelectronics and photonic integrated circuits.

Dr. Bowers is a Member of the National Academy of Engineering. He is a Fellow of the Optical Society of America (OSA) and the American Physical Society. He was a recipient of the OSA/IEEE Tyndall Award, the OSA Holonyak Prize, the IEEE LEOS William Streifer Award, and the South Coast Business and Technology Entrepreneur of the Year Award. He was a corecipient of the Electrical Engineering (EE) Times Annual Creativity in Electronics (ACE) Award for Most Promising Technology for the hybrid silicon laser in 2007.

Luke Theogarajan (M'11) received the Ph.D. degree in electrical engineering and computer science from the Massachusetts Institute of Technology, Cambridge, MA, USA, in 2007.

He is currently an Associate Professor of electrical and computer engineering with the University of California at Santa Barbara, Santa Barbara, CA, USA. He was with the Intel Corporation, Hillsboro, OR, USA, for five years, where he was part of the Pentium 4 Design Team, prior to beginning his Ph.D. degree. His research interests are low-power circuits for biological systems, high-speed circuits for optoelectronics, advanced packaging for both biosensors and electronic–photonic integration, nanoscale sensors, and supramolecular chemistry.

Prof. Theogarajan was a recipient of the 2010 National Institutes of Health (NIH) New Innovator Award and a 2011 National Science Foundation (NSF) CAREER Award. He was also the recipient of the Northrop Grumman Excellence in Teaching award in 2011, and an Outstanding Faculty Member in Electrical Engineering Award in 2009, 2010, 2011, and 2012.